DYNAMICS OF ANGELES'S QUASIMORO MOBILE ROBOT USING PRINCIPLE OF VIRTUAL POWERS

Şt. STAICU *

We report the analysis of the dynamics of a two-wheeled mobile robot of Angeles, which comprises an intermediate body. The mathematical model of the robot is formulated using the principle of virtual powers, but it is possible to verify the results in the framework of the Lagrange equations with its multipliers. The dynamic model of this mechanical system is crucial for the design and control in real-time of the robot at hand.

Lucrarea analizează dinamica unui robot mobil al lui Angeles, care este prevăzut cu două roţi şi cu un corp intermediar. Modelul matematic al robotului este formulat pe baza principiului puterilor virtuale, dar rezultatele pot fi verificate cu modelul de lucru al ecuaţiilor şi multiplicatorilor lui Lagrange. Modelul dinamic al acestui sistem mecanic este crucial pentru construcţia şi controlul mişcării robotului în timp real.

Keywords: dynamics, mobile robot, virtual powers

Introduction

Mobile robots are pre-programmable multi-functional systems designed to move material, parts, tools or specialized devices through variable programmed motions for performance of a variety of tasks. They consist of a mobile platform and some cylindrical wheels, which have a rolling with friction motion on a fixed or mobile surface.

The condition of rolling motion without slipping and side-slipping between the wheels and the contact surface demands the presence of nonholonomic constraints, which represent the kinematic model particularity of this kind of robot. The nonholonomic constraints reduce the mobile robot's instantaneous velocity degrees of freedom, and hence most robots have only two actuated joints: the two driven wheels.

Wheeled mobile robots are needed nowadays in various applications: transport for material or tools over distances much larger than their dimensions, using in inaccessible places and in some agricultural workings, entertainment robots, service robots for domestic chores and for special medical proceedings, assistive devices for the mobility-challenged and rovers for interplanetary exploration. This

* Prof., Dept. of Mechanics, University "Politehnica" of Bucharest, Romania

is why the dynamic studies of these mobile machineries acquired more and more importance.

Angeles's Quasimoro mobile robot [1] is a quasiholonomic mechanical system, which comprises two driving wheels and an intermediate body carrying the payload. The robot is currently under design, its novelty lying in the ease with which it can be controlled. The mass center of the robot is particularly placed on the vertical passing through the midpoint of the line joining the wheel centers. Moreover, in order to cope with instability, the mass center of the intermediate body is placed below the above-mentioned line.

The two main tasks of this robot are: positioning and orienting the payload, supported by the intermediate body on a flat surface (locomotion task) and stabilizing the oscillation of the intermediate body (stabilization task).

A literature survey on two-wheeled robots led to three different systems: SCOUT [2], Ginger-Segway [3] and JOE [4]. The mass center of the robot being placed below the line joining the wheel centers and non using any gyro to sense the inclination of central body, Quasimoro operates under a simpler control system than the ones of Segway and JOE.

In his paper, Angeles [9] studied some aspects of the mobile robots dynamics using the Lagrange equations. Other authors (Colbaugh et al., [11]) gave an interesting characterization of a mechanic nonholonomic system. Volterra, Appel and Ceaplighin used also the Lagrange equations and multipliers formalism in the dynamics of motion with nonholonomic constraints.

The mathematical model of a robotic mechanical system is essential to predict, in simulation, the robot dynamics and to properly design and control to robot [5], [6], [8], [12].

In the present paper we are going to establish a dynamic model for the motion of Angeles's Quasimoro mobile robot using a matrix approach. We will consider that the coordinates of mass center of the robot, the orientation angle, the angular displacements of the wheels and the rotation angle of the intermediate body determine the position and orientation of the robot.

Using the principle of virtual works, we formulate the matrix model of Quasimoro rolling robot, which represents a two-input nonlinear dynamical system with three outputs. This model is validated by means of simulations and analyses of the dynamic response of the system to different inputs and initial conditions.

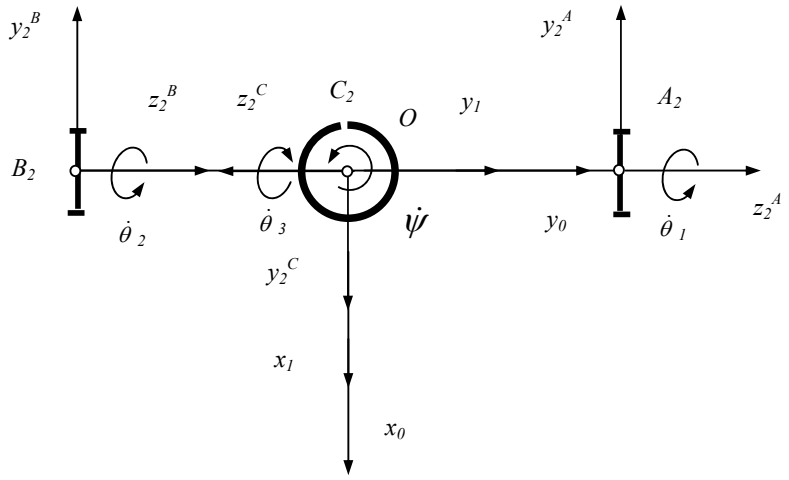

Fig. 1. Kinematical scheme of the rolling robot

The results of the analysis are very important for the robot design and control of the robot. It turns out that the major disturbance in accomplishing the two tasks at hand is caused by the oscillation of the intermediate body. Hence, the introduction of design corrections and the derivation of a suitable control algorithm should be considered in order to render the robot performance least sensitive to this disturbance.

1. Kinematics model of the robot

Quasimoro is a mobile robot consisting of two wheels of same radius r, which are actuated by two independent motors, and of an intermediate body, which contains the control equipment, the actuation system, the power supply and the transmission mechanism. The robot wheels are of conventional type according to the classification given in [7]. During motion both robot wheels can roll without slipping on a horizontal planar surface and are assumed to be permanently in contact with this surface.

A fictitious horizontal platform, attached to the frame $C_2x_1y_1z_1$ of axis C_2x_1 linking the centers of the wheels, has a planar motion [15]. Its position with respect to an inertial reference frame $Ox_0y_0z_0$, with the origin O fixed to the ground surface, is given by the coordinates x_{10}, y_{10}, r and by the orientation angle ψ, which form the following matrices

$$\vec{r}_{19}=\begin{bmatrix} x_{10} \\ y_{10} \\ r \end{bmatrix},\quad a_{10}=\begin{bmatrix} \cos\psi & \sin\psi & 0 \\ -\sin\psi & \cos\psi & 0 \\ 0 & 0 & 1 \end{bmatrix}. \tag{1}$$

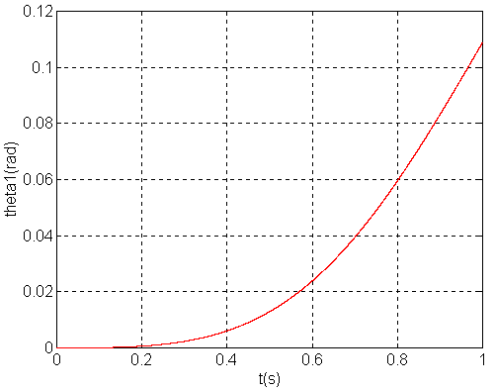

Fig. 2 Rectilinear motion: rotation angle θ_1

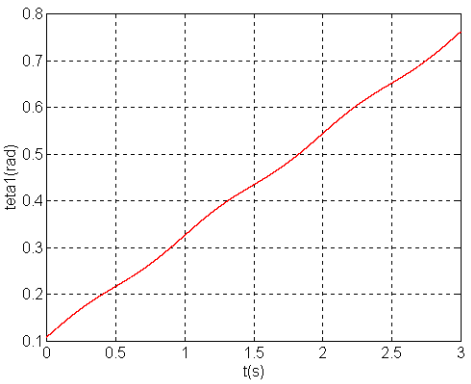

Fig. 3 Rectilinear motion: rotation angle θ_1

Two cylindrical coaxial wheels, linked to the frames $A_2x_2^Ay_2^Az_2^A$ and $B_2x_2^By_2^Bz_2^B$, are coupled to an intermediate body by means of revolute joints in points A_2 and B_2 (Fig. 1). They have known masses $m_2^A=m_2^B=m$ and the tensors of inertia

$$\hat{J}_2^A=\hat{J}_2^B=\hat{J}=\begin{bmatrix} \frac{1}{4}mr^2 & 0 & 0 \\ 0 & \frac{1}{4}mr^2 & 0 \\ 0 & 0 & \frac{1}{2}mr^2 \end{bmatrix}. \tag{2}$$

A cylinder of mass $m_2^C=M$ and tensor of inertia

$$\hat{J}_2^C=\begin{bmatrix} J_1 & 0 & 0 \\ 0 & J_2 & 0 \\ 0 & 0 & J_2 \end{bmatrix}. \tag{3}$$

is attached to the frame $C_2x_2^Cy_2^Cz_2^C$, which is centered at the midpoint C_2 of line joining the mass centers of both wheels and represent the chassis of the intermediate body.

Let us indicate with θ_i $(i=1,2)$ the rotation angles of the two wheels and with θ_3 the inclination angle of intermediate body about C_2x_1. One obtains the following transformation matrices in the mobile reference frames:

$$a_{21}^A=a_z^{\theta_1}a_1,\ a_{21}^B=a_z^{\theta_2}a_1,\ a_{21}^C=a_z^{\theta_3}a_2 \tag{4}$$

where

$$a_1 = \begin{bmatrix} 0 & 0 & -1 \\ -1 & 0 & 0 \\ 0 & 1 & 0 \end{bmatrix}, \; a_2 = \begin{bmatrix} 0 & 0 & -1 \\ 1 & 0 & 0 \\ 0 & -1 & 0 \end{bmatrix}$$

$$a_z^{\theta_i} = \begin{bmatrix} \cos\theta_i & \sin\theta_i & 0 \\ -\sin\theta_i & \cos\theta_i & 0 \\ 0 & 0 & 1 \end{bmatrix}, (i = 1, 2, 3). \tag{5}$$

Defining l the distance between the centers of the wheels, the following vectors give the relative positions of points $A_2, B_2, C_2, G_A, G_B, G_C$

$$\vec{r}_{21}^{\,A} = \begin{bmatrix} 0 \\ \frac{l}{2} \\ 0 \end{bmatrix}, \quad \vec{r}_{21}^{\,B} = \begin{bmatrix} 0 \\ -\frac{l}{2} \\ 0 \end{bmatrix}, \quad \vec{r}_{21}^{\,C} = \vec{0}$$

$$\vec{r}_2^{\,GA} = \vec{0}, \quad \vec{r}_2^{\,GB} = \vec{0}, \quad \vec{r}_2^{\,GC} = \begin{bmatrix} d \\ 0 \\ 0 \end{bmatrix}. \tag{6}$$

The kinematics of the three elements is completely characterized by the translation velocity

$$\dot{\vec{r}}_{10} = [\dot{x}_{10} \quad \dot{y}_{10} \quad 0]^T \tag{7}$$

and by the angular velocities that are given below

$$\vec{\omega}_{10} = \dot{\psi}\,\vec{u}_3, \quad \vec{\omega}_{21}^{\,A} = \dot{\theta}_1\vec{u}_3, \quad \vec{\omega}_{21}^{\,B} = \dot{\theta}_2\vec{u}_3$$
$$\vec{\omega}_{21}^{\,C} = \dot{\theta}_3\vec{u}_3, \quad \vec{u}_3 = [0 \quad 0 \quad 1]^T. \tag{8}$$

The speed difference between the wheels generates rotation of the vehicles. Moreover, differentially-driven robots can rotate on the spot.

Assuming that the two wheels roll without slipping on the surface, three analytical relations between the characteristic velocities of the two-degrees-of-freedom mobile robot express the non-holonomic constraints:

$$\vec{v}_{10} + \tilde{\omega}_{10}\vec{r}_{21}^{\,A} = [r\dot{\theta}_1 \quad 0 \quad 0]^T$$
$$\vec{v}_{10} + \tilde{\omega}_{10}\vec{r}_{21}^{\,B} = [r\dot{\theta}_2 \quad 0 \quad 0]^T, \tag{9}$$

where

$$\vec{v}_{10} = a_{10}\dot{\vec{r}}_{10} = \begin{bmatrix} \dot{x}_{10}\cos\psi + \dot{y}_{10}\sin\psi \\ -\dot{x}_{10}\sin\psi + \dot{y}_{10}\cos\psi \\ 0 \end{bmatrix}, \tilde{\omega}_{10} = a_{10}\dot{a}_{10}^T = \begin{bmatrix} 0 & -\dot{\psi} & 0 \\ \dot{\psi} & 0 & 0 \\ 0 & 0 & 0 \end{bmatrix}. \tag{10}$$

One of three analytical constrained relations (9) have been integrated:

$$\psi = \rho\,(\theta_2 - \theta_1), \quad \rho = \frac{r}{l}. \tag{11}$$

The above *conditions of connectivity* (9) can provide the expressions of Jacobian and characteristic velocities

$$\begin{aligned}\dot{\psi} &= \rho(\dot{\theta}_2 - \dot{\theta}_1)\\ \dot{x}_{10} &= \frac{r}{2}(\dot{\theta}_1 + \dot{\theta}_2)\cos\psi\\ \dot{y}_{10} &= \frac{r}{2}(\dot{\theta}_1 + \dot{\theta}_2)\sin\psi.\end{aligned} \tag{12}$$

In order to determine the relations of connectivity of accelerations we derive the matrix relations (9):

$$\begin{aligned}&\vec{\gamma}_{10} + (\tilde{\omega}_{10}\tilde{\omega}_{10} + \dot{\tilde{\omega}}_{10})\vec{r}_{21}^{\,A} =\\ &= [r\ddot{\theta}_1 \quad 0 \quad 0]^T + \tilde{\omega}_{10}[r\dot{\theta}_1 \quad 0 \quad 0]^T\\ &\vec{\gamma}_{10} + (\tilde{\omega}_{10}\tilde{\omega}_{10} + \dot{\tilde{\omega}}_{10})\vec{r}_{21}^{\,B} =\\ &= [r_1\ddot{\theta}_2 \quad 0 \quad 0]^T + \tilde{\omega}_{10}[r\dot{\theta}_2 \quad 0 \quad 0]^T,\end{aligned} \tag{13}$$

where

$$\vec{\gamma}_{10} = a_{10}\ddot{\vec{r}}_{10} = \begin{bmatrix} \ddot{x}_{10}\cos\psi + \ddot{y}_{10}\sin\psi \\ -\ddot{x}_{10}\sin\psi + \ddot{y}_{10}\cos\psi \\ 0 \end{bmatrix} \tag{14}$$

Thus, the characteristic accelerations $\ddot{\psi}$, $\ddot{x}_{10}$, $\ddot{y}_{10}$ are immediately obtained:

$$\begin{aligned}\ddot{\psi} &= \rho(\ddot{\theta}_2 - \ddot{\theta}_1)\\ \ddot{x}_{10} &= \frac{r}{2}(\ddot{\theta}_1 + \ddot{\theta}_2)\cos\psi - \frac{r\rho}{2}(\dot{\theta}_2^2 - \dot{\theta}_1^2)\sin\psi\\ \ddot{y}_{10} &= \frac{r}{2}(\dot{\theta}_1 + \dot{\theta}_2)\sin\psi + \frac{r\rho}{2}(\dot{\theta}_2^2 - \dot{\theta}_1^2)\cos\psi.\end{aligned} \tag{15}$$

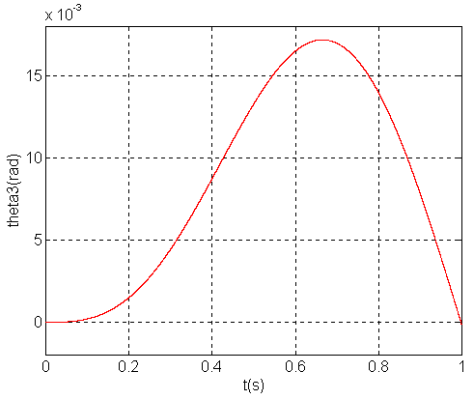

Fig. 4 Rectilinear motion: rotation angle θ_3

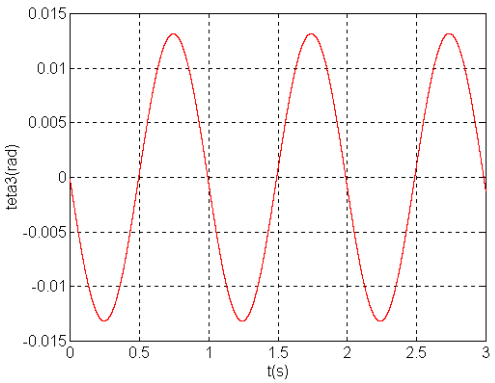

Fig. 5 Rectilinear motion: rotation angle θ_3

To describe the kinematical state of each body T_2 with respect to fixed frame $Ox_0y_0z_0$, we express the angular velocity $\vec{\omega}_{20}$ and the linear velocity $\vec{v}_{20}$ of the reference origin

$$\begin{aligned} \vec{v}_{20} &= a_{21}(\vec{v}_{10} + \tilde{\omega}_{10}\vec{r}_{21}) \\ \vec{\omega}_{20} &= a_{21}\omega_{10} + \vec{\omega}_{21}. \end{aligned} \tag{16}$$

Performing the derivatives with respect to time of the equations (17), we obtain the accelerations $\vec{\gamma}_{20}, \vec{\varepsilon}_{20}$:

$$\begin{aligned} \vec{\gamma}_{20} &= a_{21}\{\vec{\gamma}_{10} + (\tilde{\omega}_{10}\tilde{\omega}_{10} + \dot{\tilde{\omega}}_{10})\vec{r}_{21}\} \\ \vec{\varepsilon}_{20} &= a_{21}\dot{\tilde{\omega}}_{10} + \dot{\tilde{\omega}}_{21} + a_{21}\tilde{\omega}_{10}a_{21}^T\vec{\omega}_{21} \end{aligned} \tag{17}$$

and a useful square characteristic matrix (Staicu, [14])

$$\begin{aligned} \tilde{\omega}_{20}\tilde{\omega}_{20} + \dot{\tilde{\omega}}_{20} &= a_{21}\{\tilde{\omega}_{10}\tilde{\omega}_{10} + \dot{\tilde{\omega}}_{10})a_{21}^T + \\ &+ \tilde{\omega}_{21}\tilde{\omega}_{21} + \dot{\tilde{\omega}}_{21} + 2a_{21}\tilde{\omega}_{10}a_{21}^T\tilde{\omega}_{21}. \end{aligned} \tag{18}$$

2. Equations of motion

The torques $\vec{m}_1 = m_1\vec{u}_3$ and $\vec{m}_2 = m_2\vec{u}_3$, which are generated by electric motors, transmit the motion at the two wheels. Having the direction of the common axis A_2B_2, these moments can control the motion accomplished by the active wheels and the intermediate body.

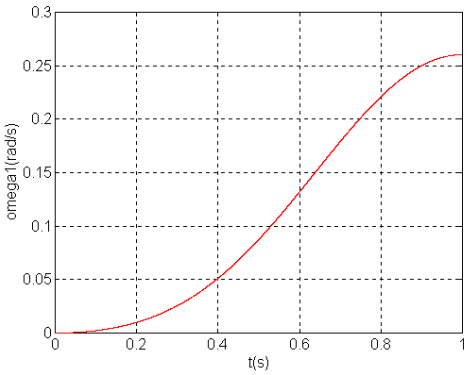

Fig. 6 Rectilinear motion: angular velocity $\dot{\theta}_1$

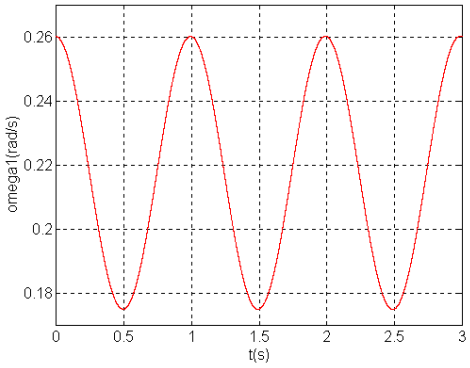

Fig. 7 Rectilinear motion: angular velocity $\dot{\theta}_1$

We will study the direct dynamic problem, in order to establish the evolution of the rotation angles $\theta_1, \theta_2, \theta_3$ and the variation of the angular velocities $\dot{\theta}_1, \dot{\theta}_2, \dot{\theta}_3$ during the transient motion of $\Delta t = 1s$ between initial position and one, which correspond to other inactivated motion, knowing the torques m_1, m_2. Thus, we will use the method of virtual powers.

Indeed, we assume that the two torque pulses of amplitudes m_1° and m_2° at an arbitrary instant are known by the functions

$$m_i(t) = m_i^\circ \sin \pi\, t\,, (i = 1,2),\ t \in [0,1], \tag{19}$$

where, for example, $m_1^\circ = 0.1\,\mathrm{Nm}$.

In every analysis, the system is considered initially at rest. It is noteworthy that the simulation runs do not account for either external dissipation such as rolling friction between the wheels and ground, and for internal dissipation, such as friction in the bearings.

The principle of virtual powers states that a mechanical system is under dynamic equilibrium if and only if the virtual powers developed by all external, internal and inertia forces vanish during any general virtual displacement, which is compatible with the kinematical constraints (Angeles, [9]; Staicu, [13]).

The force of inertia and the resultant moment of the forces of inertia have the following general form

$$\begin{aligned} -\vec{F}_{i0} &= -m_i\{\vec{\gamma}_{i0} + (\tilde{\omega}_{i0}^2 + \tilde{\varepsilon}_{i0})\vec{r}_i^{\,G}\} \\ -\vec{M}_{i0} &= -\{m_i\tilde{r}_i^{\,G}\vec{\gamma}_{i0} + \hat{J}_i\vec{\varepsilon}_{i0} + \tilde{\omega}_{i0}\hat{J}_i\vec{\omega}_{i0}\}\,, \end{aligned} \tag{20}$$

where m_i is the mass and $\hat{J}_i = \oint \tilde{r}\tilde{r}^T dm$ the tensor of inertia of rigid body T_i.

The virtual velocities of the robot bodies result from relations (9) and (17), namely:

$$\begin{aligned} &\omega_{1a}^v = 1\,,\ \omega_{2a}^v = 0,\ \omega_{3a}^v = 0,\ \omega_{10a}^v = -\rho \\ &\vec{v}_{20a}^{\,AvT} = [-r\sin\theta_1 \quad -r\cos\theta_1 \quad 0] \\ &\vec{v}_{20a}^{\,BvT} = [0 \quad 0 \quad 0] \\ &\vec{v}_{20a}^{\,CvT} = [\frac{r}{2}\sin\theta_3 \quad \frac{r}{2}\cos\theta_3 \quad 0] \\ &\vec{\omega}_{20a}^{\,AvT} = [\rho\cos\theta_1 \quad -\rho\sin\theta_1 \quad 1] \\ &\vec{\omega}_{20a}^{\,BvT} = [\rho\cos\theta_2 \quad -\rho\sin\theta_2 \quad 0] \\ &\vec{\omega}_{20a}^{\,CvT} = [\rho\cos\theta_3 \quad -\rho\sin\theta_3 \quad 0] \end{aligned} \tag{21}$$

The following expression of the torque of the couple applied to the wheel A_2 results

$$\begin{aligned} m_1 = {} & \vec{v}_{20a}^{\,AvT}\,\vec{F}_{20}^{\,A} + \vec{\omega}_{20a}^{\,AvT}\,\vec{M}_{20}^{\,A} + \vec{v}_{20a}^{\,BvT}\,\vec{F}_{20}^{\,B} + \\ & + \vec{\omega}_{20a}^{\,BvT}\,\vec{M}_{20}^{\,B} + \vec{v}_{20a}^{\,CvT}\,\vec{F}_{20}^{\,C} + \vec{\omega}_{20a}^{\,CvT}\,\vec{M}_{20}^{\,C}\,, \end{aligned} \tag{22}$$

with its analytical form

$$\begin{aligned} m_1 = {} & A_{11}\ddot{\theta}_1 + A_{12}\ddot{\theta}_2 + A_{13}\ddot{\theta}_3 + A_{14}\dot{\theta}_1\dot{\theta}_2 + \\ & + A_{15}\dot{\theta}_2\dot{\theta}_3 + A_{16}\dot{\theta}_3\dot{\theta}_1 + A_{17}\dot{\theta}_1^2 + A_{18}\dot{\theta}_2^2 + A_{19}\dot{\theta}_3^2\,, \end{aligned} \tag{23}$$

where

$$
\begin{aligned}
A_{11} &= \frac{1}{2}mr^2(3+\rho^2)+\rho^2(J_1\cos^2\theta_3+J_2\sin^2\theta_3)+\frac{1}{4}Mr^2\\
A_{12} &= -\frac{1}{2}mr^2\rho^2-\rho^2(J_1\cos^2\theta_3+J_2\sin^2\theta_3)+\frac{1}{4}Mr^2\\
A_{13} &= \frac{1}{2}Mrd\cos\theta_3\\
A_{14} &= Mrd\rho^2\sin\theta_3\\
A_{15} &= 2\rho^2(J_1-J_2)\sin\theta_3\cos\theta_3\\
A_{16} &= -2\rho^2(J_1-J_2)\sin\theta_3\cos\theta_3\\
A_{17} &= 0\\
A_{18} &= -Mrd\rho^2\sin\theta_3\\
A_{19} &= -\frac{1}{2}Mrd\sin\theta_3.
\end{aligned}
\tag{24}
$$

The relations (22) represent the *direct dynamic model* of the mobile robot motion. For the moment m_2 of the torque applied to the wheel B_2 we obtain an analogous expression:

$$
\begin{aligned}
m_2 = {} & A_{21}\ddot{\theta}_1+A_{22}\ddot{\theta}_2+A_{23}\ddot{\theta}_3+A_{24}\dot{\theta}_1\dot{\theta}_2+\\
& +A_{25}\dot{\theta}_2\dot{\theta}_3+A_{26}\dot{\theta}_3\dot{\theta}_1+A_{27}\dot{\theta}_1^2+A_{28}\dot{\theta}_2^2+A_{29}\dot{\theta}_3^2,
\end{aligned}
\tag{25}
$$

where

$$
\begin{aligned}
&A_{21}=A_{12},\ A_{22}=A_{11},\ A_{23}=A_{13}\\
&A_{24}=A_{14},\ A_{25}=A_{16},\ A_{26}=A_{15}\\
&A_{27}=A_{18},\ A_{28}=A_{17},\ A_{29}=A_{19}.
\end{aligned}
\tag{26}
$$

The third virtual displacement of the intermediate body correspond to the angular velocities

$$\omega_{3c}^v=1,\ \omega_{1c}^v=0,\ \omega_{2c}^v=0,\ \omega_{10c}^v=0. \tag{27}$$

We obtains the following differential equation

$$
\begin{aligned}
& J_2\ddot{\theta}_3+Mgd\sin\theta_3+\frac{1}{2}Mrd(\ddot{\theta}_1+\ddot{\theta}_2)\cos\theta_3+\\
& +(J_1-J_2)\rho^2(\dot{\theta}_2-\dot{\theta}_1)^2\sin\theta_3\cos\theta_3=m_1+m_2.
\end{aligned}
\tag{28}
$$

Two important maneuvers can be implemented:

1°. *Rectilinear motion*, with the angles $\psi=0,\ \theta_1=\theta_2$, two equal torques applied to the wheels

$$m_1=m_2=\frac{1}{2}(3m+M)r^2\ddot{\theta}_1+\frac{1}{2}Mrd(\ddot{\theta}_3\cos\theta_3-\dot{\theta}_3^2\sin\theta_3) \tag{29}$$

and one differential equation

$$J_2\ddot{\theta}_3+Mgd\sin\theta_3+Mrd\ddot{\theta}_1\cos\theta_3=2m_1. \tag{30}$$

2º. *Pure rotation* about the vertical axis passing through a fixed center C_2, with $\psi = -2\rho\theta_1$, $\theta_2 = -\theta_1$, $\theta_3 = 0$ and two equal torques, opposite in sign, applied to the wheels

$$m_1 = |m_2| = [mr^2(\frac{3}{2} + \rho^2) + 2\rho^2 J_1]\ddot{\theta}_1 . \tag{31}$$

3. Simulation

As application, we will analyze the motion of a rolling robot, which has the following characteristics:

$m = 0.5\,\text{kg}$, $M = 5\,\text{kg}$, $J_1 = 0.2\,\text{kgm}^2$, $J_2 = 0.4\,\text{kgm}^2$, $r = 0.3\,\text{m}$, $d = 0.2\,\text{m}$, $\rho = 0.5$.

The response of the dynamical system at hand to two different inputs has been studied. These inputs will be represented by torques pulses (19), actuating the wheels, of duration of $\Delta t = 1s$ applied at $t_0 = 0$. Each simulation takes 90 s, but most of all outputs plots will be reported in the time window that goes from 0 s to $\Delta t + 3\,\text{s}$, for example, to better show the transient response.

In every simulation the system is considered initially at rest. Two manoeuvres has been simulated: 1° rectilinear motion, while maintaining constant the orientation angle $\psi = 0$; 2° pure rotation about the vertical axis passing through C_2, with $\theta_3 = 0$, i.e. vary the orientation angle ψ only.

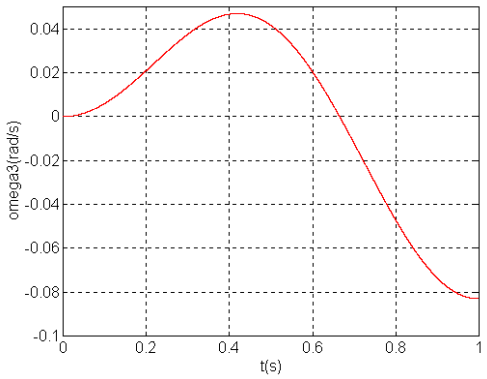

Fig. 8 Rectilinear motion: angular velocity $\dot{\theta}_3$

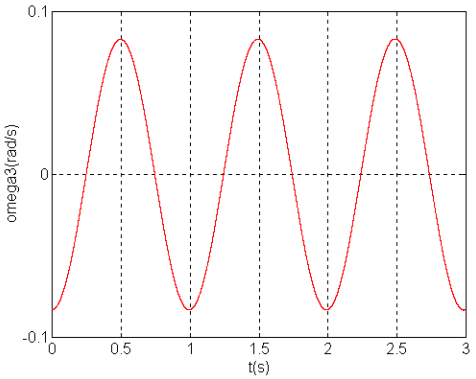

Fig. 9 Rectilinear motion: angular velocity $\dot{\theta}_3$

1°. *Rectilinear motion*

In this simulation run, two equal torque pulses (19) of amplitude $m_1^\circ = m_2^\circ = 0.1\,\text{Nm}$ are applied to the wheels.

The outputs plots are reported in the following graphs: θ_1 (Fig. 2, Fig. 3), θ_3 (Fig. 4, Fig. 5), $\dot{\theta}_1$ (Fig. 6, Fig. 7) and $\dot{\theta}_3$ (Fig. 8, Fig. 9).

The angles θ_1, θ_2 and their first derivatives are equal, since the load condition is symmetric. Moreover, we can argue that the periodic signal $\dot{\theta}_1 = \dot{\theta}_2$ (Fig. 7) is generated by $\dot{\theta}_3$.

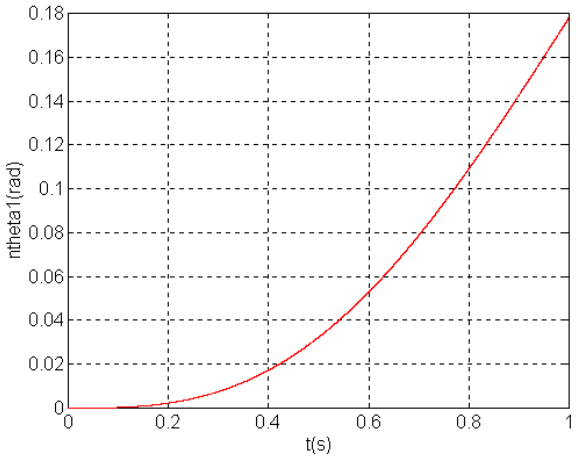

Fig. 10 Pure rotation: rotation angle θ_1

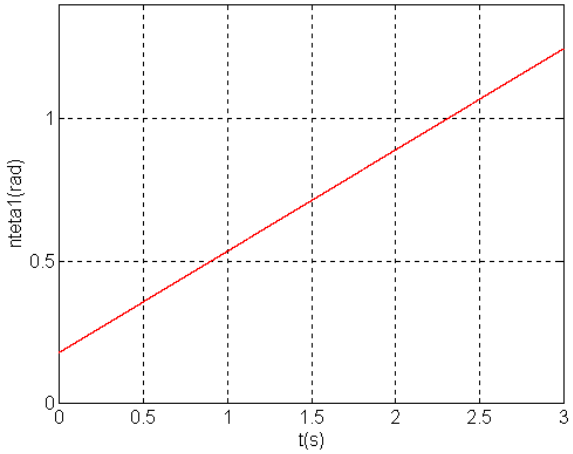

Fig. 11 Pure rotation: rotation angle θ_1

From Fig. 5, where θ_3 is represented by a periodic signal, we can infer that the oscillation of the intermediate body in the steady state is between –0.0129 rad and 0.0129 rad; of course, this theoretical oscillation needs no stabilization, since its amplitude is not big enough to be considered a disturbance for the

accomplishment of the stabilization task. However, $\theta_3(0)$ might not be zero because of assembly and manufacturing errors; moreover, the actual surface on which the robot will move can be indeed slightly inclined. Hence, it is necessary to stabilize this oscillation by a suitable control algorithm.

The rectilinear trajectory is followed with high accuracy. Of course, the wheels will never experience the same torque in reality, which calls for a suitable control algorithm for accomplishment of the locomotion task. Moreover, a control algorithm is also needed because the velocity $\dot{x}_{10} = r\dot{\theta}_1$ along the rectilinear trajectory is not constant in the steady state.

2°. *Pure rotation*

Two equal torque pulses $m_1 = -m_2 = m_1^\circ \sin \pi t$ of amplitude $m_1^\circ = 0.1\,\text{Nm}$, opposite in sign, are applied to the wheels, during $\Delta t = 1s$. The output plots are displayed in the following graphs: θ_1 (Fig. 10, Fig. 11) and $\dot{\theta}_1$ (Fig. 12, Fig. 13).

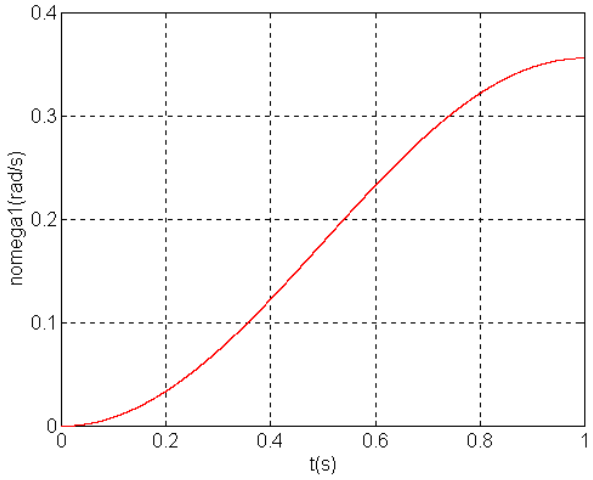

Fig. 12 Pure rotation: angular velocity $\dot{\theta}_1$

The trajectory of point C_2 reduces to a point coincident with the origin O of the inertia frame; moreover, the angular velocity will be constant in the steady state, as indicated in Fig. 13. Anyway, for what has been already stated about the errors affecting the construction of the robot, in reality the trajectory of point C_2 will not be a point; hence, a control algorithm for the accomplishment of the location task is needed.

For the assigned initial conditions and the type of input, the angle θ_3 and its first and second derivatives will remain theoretically equal to zero during the

whole simulation, while θ_1, θ_2 and their derivatives are equal in amplitude and opposite sign.

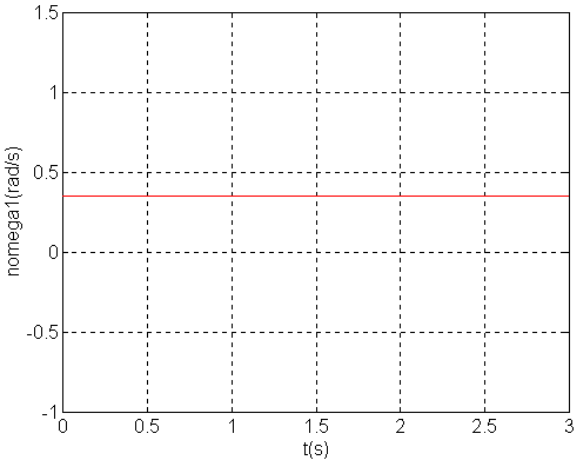

Fig. 13 Pure rotation: angular velocity $\dot{\theta}_1$

Conclusions

1°. Dynamics of Angeles's Quasimoro mobile robot, a novel quasiholonomic mechanical system, was discussed in the paper.

2°. The virtual powers method above applied, establishes three differential nonlinear equations for the rotation angles $\theta_1, \theta_2, \theta_3$.

3°. We formulated the mathematical model of the system and provided a numerical validation of it. Numerical simulations showing the dynamical behaviour of each of the system variables that need to be controlled are provided as well [10]. This work is crucial for the design and control of the system.

REFERENCES

1. *Salerno*, *A*., *Ostrovskaya, S*., *Angeles, J*., The development of quasiholonomic wheeled robots, Proceedings of the IEEE International Conference on Robotics & Automation, Washington D.C., 2002.
2. *Drenner, A., Burt, I., Dahlin, T., Kratoshvil, B., McMillen, C., Nelson, B., Papanikolopoulos, N Rybski, P.E., Stubbs, K., Waletzko, D., Berk Yesin, K.*, Mobility enhancements to the Scout robot platform, Proceedings of the IEEE International Conference on Robotics & Automation, Washington D.C., 2002.
3. *Kamen, D.J., Duggan, R.R., Field, D.J.,Heinzmann, R.K., Amsbury, B., Langenfeld, C.C*., Personal mobility vehicles and methods, *Patent*, PCT/US00/15144, 2000.
4. *Grasser, F., D'Arrigo, A., Colombi, S., Rufer, A.C*., JOE: A mobile, inverted pendulum, IEEE Transaction on Industrial Electronics, 49 (1), pp. 107-114, 2002.
5. *Salerno, A., Angeles, J*., On the nonlinear Controllability of a Quasiholonomic Mobile Robot, Technical report, Department of Mechanical Engineering, McGill University, Montreal, Canada, August 2002.

6. *Saha, S.K., Schiehlen,W.O.,* Recursive kinematics and dynamics for parallel structured closed-loop multibody systems, Mech. Struct. & Mach., 29 (2), pp. 143-175, 2001.
7. *Muir,P.F., Neuman, C.P*., Kinematic modeling of mobile robots, Journal of Robotic Systems, 4 (2), pp. 281-304. 1987.
8. *Ostrovskaya, S., Angeles, J.,* Nonholonomic systems revisited within the framework of analytical mechanics, Applied Mechanics Reviews, 51 (7), pp. 415-433, 1998.
9. *Angeles, J.,* Fundamentals of Robotic Mechanical Systems. Theory, Methods and Algorithms, Springer-Verlag, New York, 1997.
10. *SIMULINK,* Dynamic System Simulation Software, Natick, MA: The Math Works Inc., 1995.
11. *Colbaugh, R., Trabatti, M., Glass, K*., Redundant nonholonomic mechanical system. Characterization and control, Robotica, Vol. 17, 1999.
12. *Velinski, S.A., Gardner,J.E.,* Kinematics of Mobile manipulator and implications for design, Journal of Robotic Systems, Vol. 17, 6, 2000.
13. *Staicu, Şt*., Mecanica teoretica, Edit. Didactica & Pedagogica, Bucureşti, 1998.
14. *Staicu, Şt*., Méthodes matricielles en dynamique des mécanismes, Scientific Bulletin, Series D, Mechanical Engineering, University "Politehnica" of Bucharest, 62, 3, 2000.
15. *Staicu, St., Carp-Ciocardia, D.C.,* Dynamics of Mobile Robots, Proceedings of the 13th International DAAAM Symposiun, Vienna, Austria, 2002.
16. *Staicu, Şt., Carp-Ciocardia, D.C*., Dynamic Analysis of Clavel's Delta Parallel Robot, Proceedings of the IEEE International Conference on Robotics & Automation, Taipei, Taiwan, 2003.